Preprints of the
15th IFAC Symposium on System Identification
Saint-Malo, France, July 6-8, 2009

Decoupling Identification for Serial Two-link Robot Arm with Elastic Joints

Junji Oaki [*,**] **Shuichi Adachi** [**]

[*] *Corporate Research and Development Center, Toshiba Corporation Kawasaki, Japan (e-mail: junji.ooaki@toshiba.co.jp).*
[**] *Faculty of Science and Technology, Keio University Yokohama, Japan (e-mail: adachi@appi.keio.ac.jp).*

Abstract: The objective of our study is to build a precise model by applying the technique of system identification for the model-based control of a nonlinear robot arm, taking joint-elasticity into consideration. This paper proposes a systematic identification method, called "decoupling identification", for a serial two-link robot arm with elastic joints caused by the Harmonic drive® reduction gears. The proposed method serves as an extension of the conventional rigid-joint-model-based identification. The robot arm is treated as a serial two-link two-inertia system with nonlinearity. The decoupling identification method using link-accelerometer signals enables the serial two-link two-inertia system to be divided into two linear one-link two-inertia systems. The MATLAB®'s commands for state-space model estimation are utilized in the proposed method. Physical parameters such as motor inertias, link inertias, joint-friction coefficients and joint-spring coefficients are estimated through the identified one-link two-inertia systems. Experimental results using a SCARA-type planar two-link robot arm with elastic reduction gears showed an accuracy of the proposed identification method.

Keywords: Robot arms; Nonlinear systems; Mechanical resonance; Frequency response; Multivariable systems; Closed-loop identification; Nonlinear optimization; MATLAB.

1. INTRODUCTION

The industrial robots with serial links, called SCARA (Selective Compliant Assembly Robot Arm) or PUMA (Programmable Universal Manipulation Arm), are widely used. Nowadays, the robots are required to be controlled with high acceleration and suppressed vibration. The dynamic model-based control considering the joint-elasticity of the robot (Ott (2008)) is necessary in order to satisfy this requirement. Although rigid-joint-model-based identification has been researched for the last two decades (Khalil et al. (2002)), the field of elastic-joint-model-based identification is still in its infancy. Albu-Schäffer et al. (2001) showed an simple identification method for a 7dof elastic-joint robot using joint torque sensors, motor encoders, link encoders and motor brakes. However, coupled vibration effects caused by the elastic joints are not considered.

The objective of our study is to build a precise model by applying the technique of system identification for the model-based control of a nonlinear robot arm, taking joint-elasticity into consideration. This paper proposes a systematic identification method, called "decoupling identification", for a serial two-link robot arm with elastic joints caused by the Harmonic drive® reduction gears. The proposed method serves as an extension of the conventional rigid-joint-model-based identification. The robot arm is treated as a serial two-link two-inertia system with nonlinearity. The decoupling identification method using link-accelerometer signals enables the serial two-link two-inertia system to be divided into two linear one-link two-inertia systems. The MATLAB®'s commands for state-space model estimation are utilized in the proposed method. Physical parameters such as motor inertias, link inertias, joint-friction coefficients and joint-spring coefficients are estimated through the identified one-link two-inertia systems.

In the sequel, the proposed "decoupling identification" method is described in detail. Experiments using a SCARA-type planar two-link robot arm with elastic reduction gears are conducted to show an accuracy of the proposed identification method.

2. TARGET SYSTEM

In this paper, a controlled object is the planar serial two-link robot arm with elastic joints shown in Fig. 1. A DC motor drives each joint with the Harmonic drive® gear that behaves as an elastic spring element. The Harmonic drive® has nonlinear spring characteristics approximated by three linear spring coefficients shown in Fig. 2. The arm mechanism is similar in structure to the SCARA robot's 1st and 2nd links. This means that two one-link two-inertia systems are located in series. The authors call the mechanism a "serial two-link two-inertia system" (Oaki et al. (2008)). The drive systems for the 1st and 2nd joints have identical structures. However, the 2nd joint performs not only rotational motion but also translational motion. The coupled vibrational characteristics of the 2nd joint are more complicated than those of the 1st joint.

Payloads made of five brass disks (1 kg per disk) are attached at the tip of the 2nd link. The payloads can

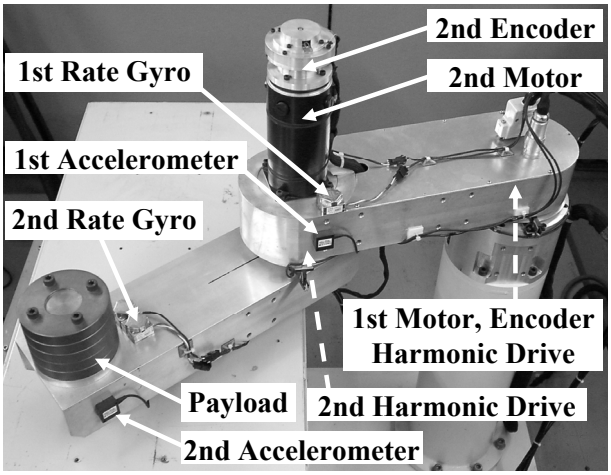

Fig. 1. Planar serial two-link robot arm with elastic joints.

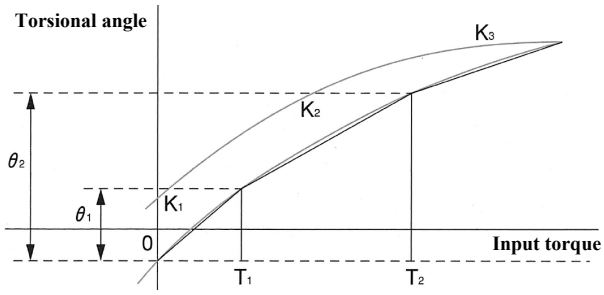

Fig. 2. Nonlinear chacteristics of Harmonic drive®.

be changed in the range of 5 kg to 0 kg. Each motor has a built-in rotary encoder for measuring the motor rotation angle. An accelerometer (bandwidth : 300 Hz) for measuring the link translational acceleration is mounted on each link. Angular acceleration of each link is computed by the coordinate transformation. Angular velocity of each link is computed by the sensor-fusion operation using the difference of the encoder signal with a low-pass filter and the integration of the angular acceleration signal with a high-pass filter, described below. A rate gyro (bandwidth : 5 Hz) mounted on each link is only used for testing the accuracy of the link-angular-velocity computation.

The link angular accelerations and velocities are utilized for computing the nonlinear interaction torques between two links. The link angular velocities in addition to the motor angular velocities are useful for improving identification accuracy. A real-time Linux PC is utilized for arm control and the data collection for identification.

3. DYNAMIC MODEL OF SERIAL TWO-LINK TWO-INERTIA SYSTEM

The dynamic model of the serial two-link two-inertia system (Ott (2008)) is given by

$$\begin{aligned}&\boldsymbol{M}_M\ddot{\boldsymbol{\theta}}_M + \boldsymbol{D}_M\dot{\boldsymbol{\theta}}_M + \boldsymbol{f}_M\mathrm{sgn}(\dot{\boldsymbol{\theta}}_M)\\ &= \boldsymbol{E}\boldsymbol{u} - \boldsymbol{N}_G[\boldsymbol{K}_G(\boldsymbol{N}_G\boldsymbol{\theta}_M - \boldsymbol{\theta}_L)\\ &\qquad + \boldsymbol{D}_G(\boldsymbol{N}_G\dot{\boldsymbol{\theta}}_M - \dot{\boldsymbol{\theta}}_L)] \qquad (1)\\ &\boldsymbol{M}_L(\boldsymbol{\theta}_L)\ddot{\boldsymbol{\theta}}_L + \boldsymbol{c}_L(\dot{\boldsymbol{\theta}}_L,\boldsymbol{\theta}_L) + \boldsymbol{D}_L\dot{\boldsymbol{\theta}}_L\\ &= \boldsymbol{K}_G(\boldsymbol{N}_G\boldsymbol{\theta}_M - \boldsymbol{\theta}_L) + \boldsymbol{D}_G(\boldsymbol{N}_G\dot{\boldsymbol{\theta}}_M - \dot{\boldsymbol{\theta}}_L) \qquad (2)\end{aligned}$$

$\boldsymbol{\theta}_M = [\theta_{M1}, \theta_{M2}]^T$: motor rotation angle (1, 2 : link number)
$\boldsymbol{\theta}_L = [\theta_{L1}, \theta_{L2}]^T$: link rotation angle
$\boldsymbol{M}_L(\boldsymbol{\theta}_L) \in R^{2\times 2}$: link inertia matrix
$\boldsymbol{c}_L(\dot{\boldsymbol{\theta}}_L, \boldsymbol{\theta}_L) \in R^{2\times 1}$: Coriolis and centrifugal force vector
$\boldsymbol{M}_M = \mathrm{diag}(m_{M1}, m_{M2})$: motor-side inertia
$\boldsymbol{D}_M = \mathrm{diag}(d_{M1}, d_{M2})$: motor-side viscous friction coefficient
$\boldsymbol{D}_L = \mathrm{diag}(d_{L1}, d_{L2})$: link-side viscous friction coefficient
$\boldsymbol{K}_G = \mathrm{diag}(k_{G1}, k_{G2})$: gear-spring coefficient
$\boldsymbol{D}_G = \mathrm{diag}(d_{G1}, d_{G2})$: gear-dumping coefficient
$\boldsymbol{N}_G = \mathrm{diag}(n_{G1}, n_{G2})$: gear-reduction ratio $(n_{G1},\ n_{G2} \le 1)$
$\boldsymbol{f}_M = [f_{M1}, f_{M2}]^T$: motor-side Coulomb friction torque
$\boldsymbol{E} = \mathrm{diag}(e_1, e_2)$: torque / input-voltage coefficient
$\boldsymbol{u} = [u_1, u_2]^T$: input voltage (motor-current control reference).

The link inertia matrix is given by

$$\boldsymbol{M}_L(\boldsymbol{\theta}_L) = \begin{bmatrix}\alpha+\beta+2\gamma\cos(\theta_{L2}) & \beta+\gamma\cos(\theta_{L2})\\ \beta+\gamma\cos(\theta_{L2}) & \beta\end{bmatrix}, \qquad (3)$$

where α, β, and γ are the base dynamic parameters (Khalil et al. (2002)) of the two-link robot arm. For convenience, $m_{L1} \equiv \alpha+\beta+2\gamma$ is defined for the maximum value of the element $(1,1)$ in the link inertia matrix. Also, $m_{L2} \equiv \beta$ is defined for the constant value of the element $(2,2)$.
The Coriolis and centrifugal force vector is given by

$$\boldsymbol{c}_L(\dot{\boldsymbol{\theta}}_L, \boldsymbol{\theta}_L) = \begin{bmatrix}-\gamma(2\dot{\theta}_{L1}\dot{\theta}_{L2} + \dot{\theta}_{L2}^2)\sin(\theta_{L2})\\ \gamma\dot{\theta}_{L1}^2\sin(\theta_{L2})\end{bmatrix}. \qquad (4)$$

Since the torsional angles of the elastic joints are very small, the trigonometric functions $\cos(\theta_{L2})$ and $\sin(\theta_{L2})$ can be computed using the approximation $\theta_{L2} = n_{G2}\theta_{M2}$. This paper proposes an accurate estimation method for the physical parameters that appear in (1) and (2). It is necessary to estimate β and γ previously for the proposed method. Therefore, the rigid-joint model is required using the approximation $\boldsymbol{\theta}_M = \boldsymbol{N}_G^{-1}\boldsymbol{\theta}_L$ in (1) and (2) as

$$\begin{aligned}&\boldsymbol{M}(\boldsymbol{\theta}_L)\ddot{\boldsymbol{\theta}}_L + \boldsymbol{c}_L(\dot{\boldsymbol{\theta}}_L,\boldsymbol{\theta}_L) + \boldsymbol{D}\dot{\boldsymbol{\theta}}_L\\ &\qquad + \boldsymbol{f}_M\mathrm{sgn}(\dot{\boldsymbol{\theta}}_M)\boldsymbol{N}_G^{-1} = \boldsymbol{E}\boldsymbol{u}\boldsymbol{N}_G^{-1} \qquad (5)\\ &\boldsymbol{M}(\boldsymbol{\theta}_L) =\\ &\begin{bmatrix}\alpha+\beta+2\gamma\cos(\theta_{L2}) + m_{M1}/n_{G1}^2 & \beta+\gamma\cos(\theta_{L2})\\ \beta+\gamma\cos(\theta_{L2}) & \beta+m_{M2}/n_{G2}^2\end{bmatrix} \qquad (6)\\ &\boldsymbol{D} = \mathrm{diag}(d_{L1}+d_{M1}/n_{G1}^2,\ d_{L2}+d_{M2}/n_{G2}^2), \qquad (7)\end{aligned}$$

where $\boldsymbol{M}(\boldsymbol{\theta}_L)$ and $\boldsymbol{D}$ are the inertia matrix and viscous-friction coefficient matrix respectively. The parameters in (5) can be estimated by the conventional rigid-joint-model-based identification method (Khalil et al. (2002)).

4. SIGNAL PROCESSING FOR MEASURING LINK-SIDE STATE VARIABLES

Each of the link angular accelerations is computed by the coordinate transformation of the link translational accelerations using the accelerometer signals as

$$\begin{aligned}\ddot{\theta}_{L1} =& \frac{a_1}{l_{a1}} \qquad (8)\\ \ddot{\theta}_{L2} =& \frac{a_2}{l_{a2}} - \frac{a_1}{l_{a1}} - \frac{a_1}{l_{a2}}\cos(n_{G2}\theta_{M2})\\ &- \frac{l_{a1}}{l_{a2}}\dot{\theta}_{L1}^2\sin(n_{G2}\theta_{M2}) \qquad (9)\end{aligned}$$

where a_1, a_2: link angular acceleration (1, 2 : link number)
l_{a1}, l_{a2}: mouting distance of accelerometer from each joint.

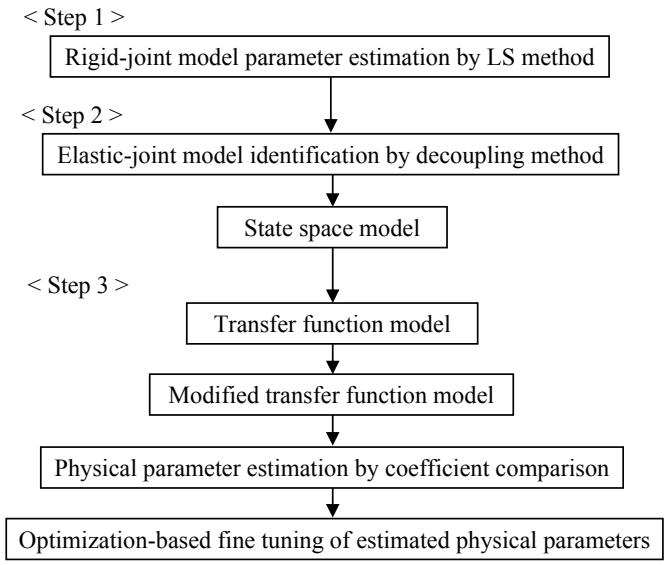

Fig. 3. Outline of the proposed identification method.

Each of the link angular velocities is computed by the sensor fusion operation using the difference of the encoder signal with a low-pass filter $G_L(s) = 1/(1 + T_V s)$ and the integration of the angular acceleration signal with a high-pass filter $G_H(s) = 1 - G_L(s)$ as

$$\dot{\theta}_{Li} = \frac{1}{1 + T_V s}(\dot{\theta}_{Mi} + T_V \ddot{\theta}_{Li}) \quad (i = 1, 2) \tag{10}$$

where T_V is a time constant for low-pass and high-pass filters.

5. DECOUPLING IDENTIFICATION PROCEDURE FOR SERIAL TWO-LINK TWO-INERTIA SYSTEM

The proposed identification method enables the serial two-link two-inertia system (1) and (2) to be divided into two linear one-link two-inertia systems. The method consists of the three steps shown in Fig. 3. The first step is the physical parameter estimation for the rigid-joint model. The second step is the state-space model estimation for each of the links based on the elastic-joint model. The third step is the physical parameter estimation for the elastic-joint model via two single-input single-output transfer functions converted from the state-space models. It is assumed that the nonlinear spring coefficient can be estimated as a linear parameter with constant-amplitude input using a pseudo random binary signal (PRBS). For example, the maximum spring coefficient K_3 shown in Fig. 2 can be estimated with a large amplitude PRBS.

5.1 Physical parameter estimation for rigid-joint model

It is necessary to estimate β and γ in (5) previously for the proposed method. The conventional rigid-joint-model-based identification using the least-squares method (Khalil et al. (2002)) can be applied to estimate the physical parameters in (5) using arbitrary motion data of the two-link robot arm. The nonlinear interaction torques between two links are computable using the estimated $\hat{\beta}$ and $\hat{\gamma}$ and the link angular accelerations and velocities. This fact plays an important role in the proposed decoupling identification method. The estimated Coulomb friction torque should be removed from the motor input data for the state-space model estimation in the next subsection.

5.2 State-space model estimation for elastic-joint model

The proposed decoupling identification method enables the serial two-link two-inertia system (1) and (2) to be divided into two linear one-link two-inertia systems. Using (1) and (2), the state-space model expression for the 1st joint is obtained as

$$\dot{\boldsymbol{x}}_1 = \boldsymbol{A}_1 \boldsymbol{x}_1 + \boldsymbol{B}_1 \begin{bmatrix} u_1 \\ \tau_1 \end{bmatrix}, \ \boldsymbol{A}_1 \in R^{4\times 4}, \ \boldsymbol{B}_1 \in R^{4\times 2} \tag{11}$$

$$\boldsymbol{y}_1 = \boldsymbol{C}_1 \boldsymbol{x}_1, \quad \boldsymbol{C}_1 \in R^{2\times 4} \tag{12}$$

$$\boldsymbol{x}_1 \equiv [\theta_{M1}, \ \theta_{L1}, \ \dot{\theta}_{M1}, \ \dot{\theta}_{L1}]^T$$

$$\boldsymbol{y}_1 \equiv [\dot{\theta}_{M1}, \ \dot{\theta}_{L1}]^T$$

$$\tau_1 = -(\hat{\beta} + \hat{\gamma}\cos(\theta_{L2}))\ddot{\theta}_{L2} + \hat{\gamma}(2\dot{\theta}_{L1}\dot{\theta}_{L2} + \dot{\theta}_{L2}^2)\sin(\theta_{L2}), \tag{13}$$

where τ_1 is the nonlinear interaction torque from the 2nd link, computed using the link angular accelerations and velocities. The MATLAB®'s "pem" or "n4sid" command (Ljung (2007)) is applicable to estimate the state-space model (11) and (12). The estimated model has two inputs, two outputs and four state variables. In this case, the motor input u_1 and the computed torque τ_1 are employed as inputs for linearizing and decoupling in the multi-input identification. Furthermore, the link and motor angular velocity are employed as outputs for improving accuracy in the multi-output identification.

It is required that the element $(1, 1)$ in (3) is constant during the motion for the linear estimation commands. It is also required for τ_1 to have "frequency richness condition" for accurate identification. Therefore, it is necessary to investigate the element $(1, 1)$ in (3), and the power spectral density of τ_1 using experimental data. It is the same deriving procedure for the 2nd joint using (1) and (2). The nonlinear interaction torque from the 1st link can be computed using the link angular accelerations and velocities as

$$\tau_2 = -(\hat{\beta} + \hat{\gamma}\cos(\theta_{L2}))\ddot{\theta}_{L1} - \hat{\gamma}\dot{\theta}_{L1}^2 \sin(\theta_{L2}). \tag{14}$$

5.3 Physical parameter estimation for elastic-joint model

Four single-input single-output transfer functions are obtained by converting from the state-space model (11) and (12) for the 1st joint as

$$\dot{\theta}_{M1}(s) = G_{11}(s)\, u_1 + G_{12}(s)\, \tau_1 \tag{15}$$

$$\dot{\theta}_{L1}(s) = G_{21}(s)\, u_1 + G_{22}(s)\, \tau_1. \tag{16}$$

The transfer function $G_{11}(s)$ from motor input u_1 to motor angular velocity $\dot{\theta}_{M1}$ is expressed using the six physical parameters as

$$G_{11}(s) = \frac{b_0 + b_1 s + b_2 s^2}{a_0 + a_1 s + a_2 s^2 + a_3 s^3} \tag{17}$$

where
$$a_0 = d_{M1} + n_{G1}^2 d_{L1}$$
$$a_1 = m_{M1} + n_{G1}^2 m_{L1} + (n_{G1}^2 d_{G1} d_{L1} + d_{M1} d_{L1} + d_{M1} d_{G1})/k_{G1}$$
$$a_2 = (m_{M1} d_{L1} + m_{M1} d_{G1} + m_{L1} d_{M1} + n_{G1}^2 m_{L1} d_{G1})/k_{G1}$$
$$a_3 = m_{M1} m_{L1}/k_{G1}$$
$$b_0 = 1, \ b_1 = (d_{L1} + d_{G1})/k_{G1}, \ b_2 = m_{L1}/k_{G1}.$$

A set of six simultaneous equations is obtained by the coefficient comparison using (17) and the transfer function conversion from the estimated state-space model by the subspace identification method. The six physical parameters are obtained by solving the simultaneous equations.

However, when the sampling rate for identification is selected to be fast for estimating the vibrational characteristics caused by the elastic joints, the results in the low-frequency region may be inaccurate. In order to modify the low-frequency region of the estimated transfer function (17), the first-order lag element of the denominator is replaced using the estimated physical parameters for the rigid-joint model above as

$$G_{11}(s) = \frac{b_0 + b_1 s + b_2 s^2}{(c_0 + c_1 s)(d_0 + d_1 s + d_2 s^2)} \qquad (18)$$

where $c_0 = d_{M1} + n_{G1}^2 d_{L1},\ c_1 = m_{M1} + n_{G1}^2 m_{L1},\ d_0 = 1.$ This approximation is valid when the cut-off frequency of the first-order lag element is low enough compared with the frequency of the vibrational characteristics. The six physical parameters for the 1st joint are now obtained by solving (17) and (18). It is the same deriving procedure for the 2nd joint.

Furthermore, fine tuning of the estimated physical parameters is performed using closed-loop simulations with the nonlinear least-squares optimization (Mathworks (2007)). The parameter-search ranges are set to be small to ensure the convergence. All physical parameters are simultaneously optimized except the coulomb friction torque because of its nonlinearity.

6. EXPERIMENTAL RESULTS AND DISCUSSIONS

The proposed decoupling identification method was verified through experiments performed using the SCARA-type planar two-link robot arm with 5 kg payload (Fig. 1).

Firstly, the physical parameter estimation for the rigid-joint model was performed. Secondly, a PRBS was applied to the 1st joint by open-loop control as input data for identification while the 2nd joint was free because of no control. The sampling time for input and output data was set to 0.025 ms. Since the PRBS (period : 1023) was produced at 1 ms intervals, data collection continued for 1.023 s. The sampling time 1 ms was changed to 2 ms using decimation. The PRBS amplitude was set to 10.0 V (maximum). These identification conditions were determined by some trial and error. Fig. 4 shows the PRBS input data (first 0.3 s of 1.023 s). Fig. 5 shows nonlinear interaction torque data and its power spectral density. Although the spectral density is somewhat bumpy, it is satisfactory in practice as another input data for multi-input identification. It was checked the cosine of the 2nd link angle was changing with value of 0.999 or more, during the 1st link motion for identification. Therefore, the element $(1, 1)$ in (3) is regarded as constant.

Two-input two-output state-space model can be estimated using the input and output data by the MATLAB®'s "pem" command (Ljung (2007)). In Fig. 6, the solid lines show the estimated frequency response from motor input u_1 to motor angular velocity $\dot{\theta}_{M1}$. The vibrational characteristics of a one-link two-inertia system such as (17) are shown. In Fig. 6, the lines show the frequency response after the modification using (18). Fig. 7 shows the optimization-based fine tuning of the estimated physical parameters using the 1st-link angular-velocity step responses of the real arm and simulation. In Fig. 6, the chain lines show the optimized frequency response after the nonlinear least-squares optimization (Mathworks (2007)).

Fig. 8 shows examples for model accuracy validation using velocity step responses for the 1st link. The good agreement between the real arm and simulation using the estimated physical parameters demonstrates the accuracy of the proposed decoupling identification method. Also, Fig. 9 shows the typical vibrational characteristics of the one-link two-inertia system for the 2nd link.

In Fig. 10, the solid lines estimated by the proposed decoupling identification method, using the computed torques and motor inputs, show the typical characteristics of the one-link two-inertia systems. The dashed lines estimated by the method that utilizes only motor inputs cannot express the characteristics because of the interaction torques. These phenomena are remarkable at the 2nd link.

Fig. 11 shows effective examples for multi-output identification for the 1st link under changing payload (5 kg–0 kg). The right-hand figures in Fig. 11 show the 2-output identification using the link angular velocity in addition to the motor angular velocity faithful to payload changing.

Next, a PRBS was applied to the 1st (2nd) joint by open-loop control as input data for identification while the 2nd (1st) joint was locked by closed-loop control using PI velocity servos. Fig. 12 shows nonlinear interaction torque data and its power spectral density. Although the spectral density is small in the low-frequency region compared with Fig. 5, the left-hand figures in Fig. 13 show the proposed method also works as closed-loop identification using the "pem" command. As opposed to it, the right-hand figures in Fig. 13 show inaccurate results using the "n4sid" command. The "pem" command is powerful because of the iterative prediction-error minimization based on the initial state-space model estimated using the "n4sid" command.

Finally, Fig. 14 shows the variations of the estimated frequency responses under changing the PRBS-input amplitude. Fig. 15 also shows the plots for squares of the estimated anti-resonant angular frequency under changing the PRBS-input amplitude. This "square" operation is because of the fact that the anti-resonance frequency is proportional to square-root of the joint-spring coefficient. These figures demonstrate the nonlinear characteristics of the Harmonic drive® shown in Fig. 2.

7. CONCLUSION

Experimental results using a SCARA-type planar two-link robot arm with elastic reduction gears show the accuracy of the proposed "decoupling identification" method. The precise model is obtained by applying the technique of system identification for the model-based control of a nonlinear robot arm, taking joint-elasticity into consideration. Although the method was prepared as open-loop identification, it was found that the method also worked as closed-loop identification in this paper. Therefore, it is applicable to a PUMA-type vertical two-link robot arm which needs to maintain the link-posture under gravity.

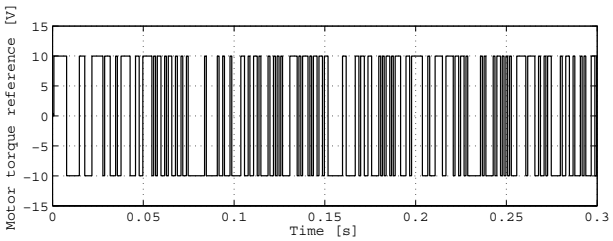

Fig. 4. Pseudo random binary signal (PRBS) input data for 1st link identification (first 0.3 s of 1.023 s).

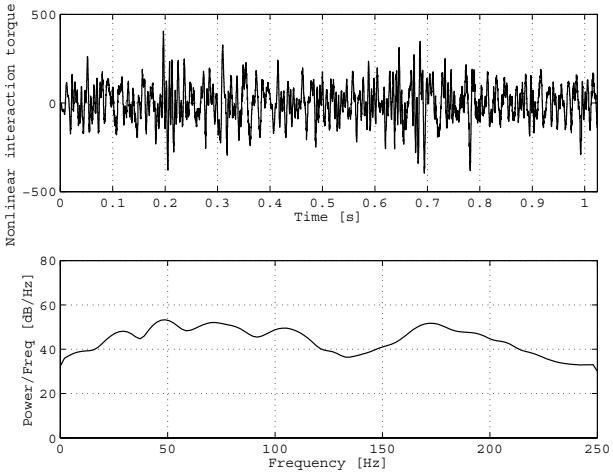

Fig. 5. Nonlinear interaction torque data for 1st link identification and its power spectral density, where 2nd link is free.

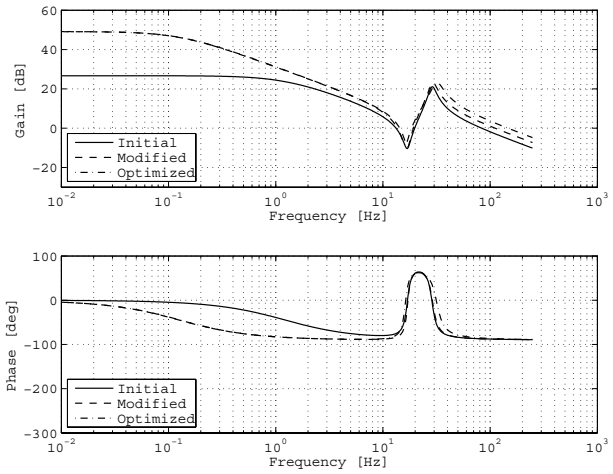

Fig. 6. Modification and optimization of initial estimated frequency responses for 1st link from motor input u_1 to motor angular velocity $\dot{\theta}_{M1}$.

REFERENCES

A.Albu-Schäffer and G.Hirzinger. Parameter identification and passivity based joint control for a 7dof torque controlled light weight robot. *Proc. IEEE International Conference on Robotics and Automation*, pages 1087–1093, 2001.

W.Khalil and E.Dombre. Modeling, Identification & Control of Robots. *Kogan Page Science*, 2002.

L.Ljung. System Identification Toolbox for Use with MATLAB (Version 7.0). *The MathWorks*, 2007.

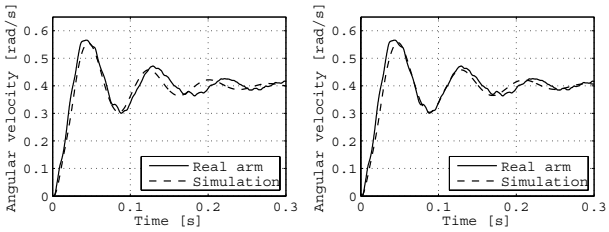

Fig. 7. Optimization-based fine tuning of estimated physical parameters using 1st link angular velocity step responses. Left: Before optimization. Right: After optimization.

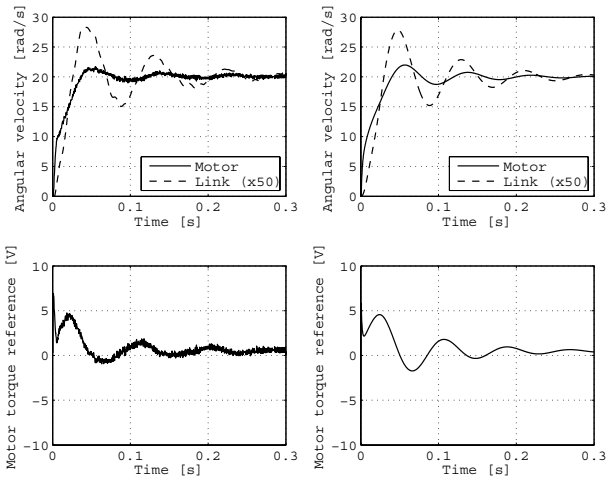

Fig. 8. Examples for model accuracy validation using velocity step responses for 1st link. Left: Real arm. Right: Simulation.

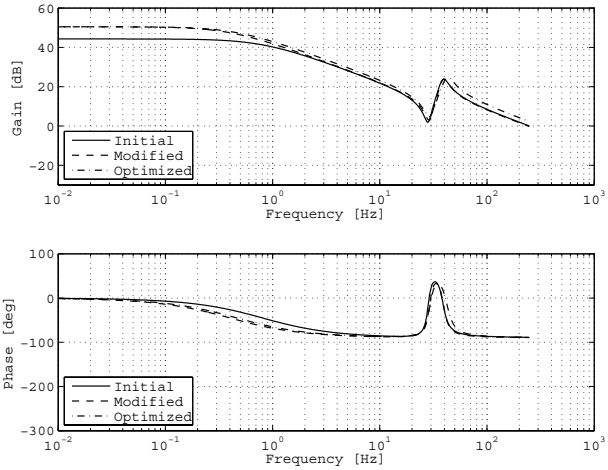

Fig. 9. Modification and optimization of initial estimated frequency responses for 2nd link from motor input u_2 to motor angular velocity $\dot{\theta}_{M2}$.

The MathWorks. Optimization Toolbox for Use with MATLAB (Version 3.1.1). *The MathWorks*, 2007.

J.Oaki and S.Adachi. Decoupling Identification and Physical Parameter Estimation for Serial Two-link Two-inertia System. *IEEJ Trans. IA*, Vol.128, No.5, pages 669–677, 2008 (in Japanese).

C.Ott. Cartesian Impedance Control of Redundant and Flexible-Joint Robots. *Springer*, 2008.

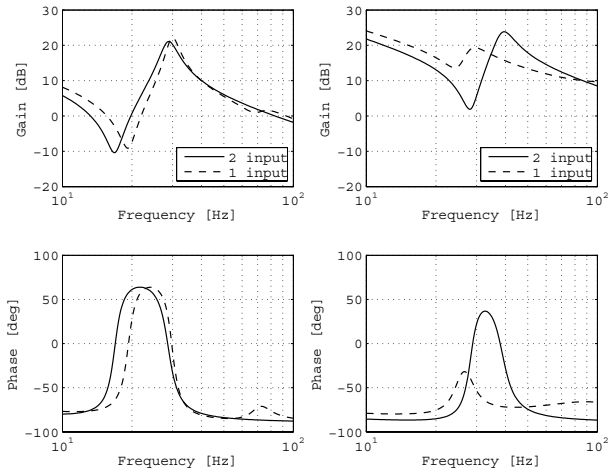

Fig. 10. Effective examples for decoupling identification from motor input to motor angular velocity. Left: 1st link. Right: 2nd link.

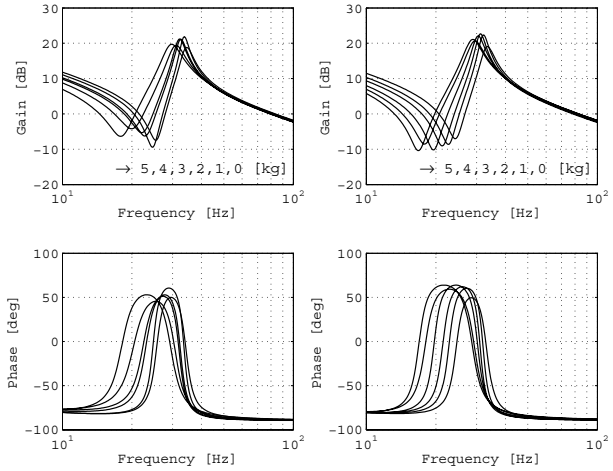

Fig. 11. Effective examples for multi-output identification for 1st link under changing payload. Left: 1 output. Right: 2 outputs.

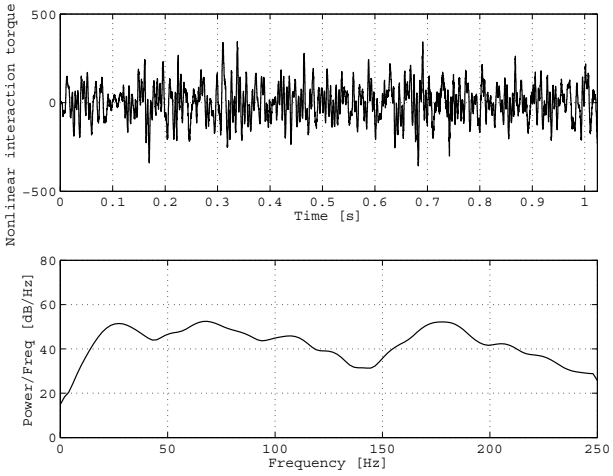

Fig. 12. Nonlinear interaction torque data for 1st link identification and its power spectral density, where 2nd link is closed-loop controlled.

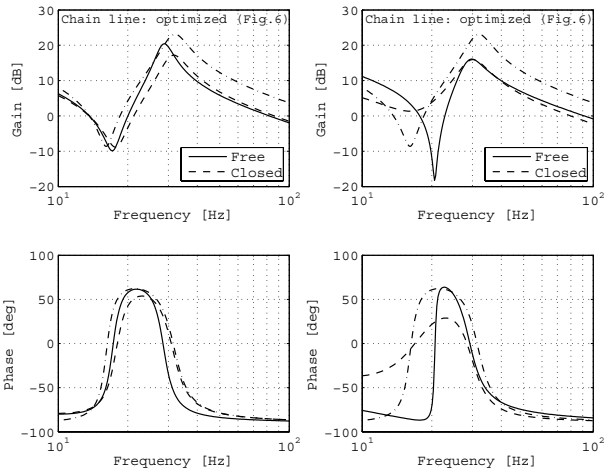

Fig. 13. Closed-loop effects against estimated frequency responses from 1st motor input to motor angular velocity, where 2nd link is free or closed-loop controlled. Left: "pem" command. Right: "n4sid" command.

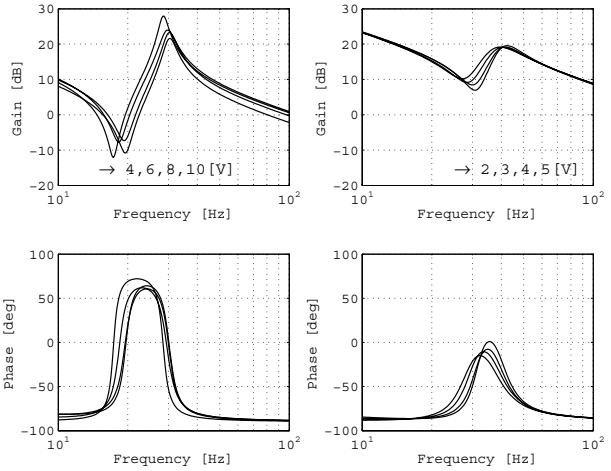

Fig. 14. Variations of estimated frequency responses under changing PRBS-input amplitude, where payload is 3 kg. Left: 1st link. Right: 2nd link.

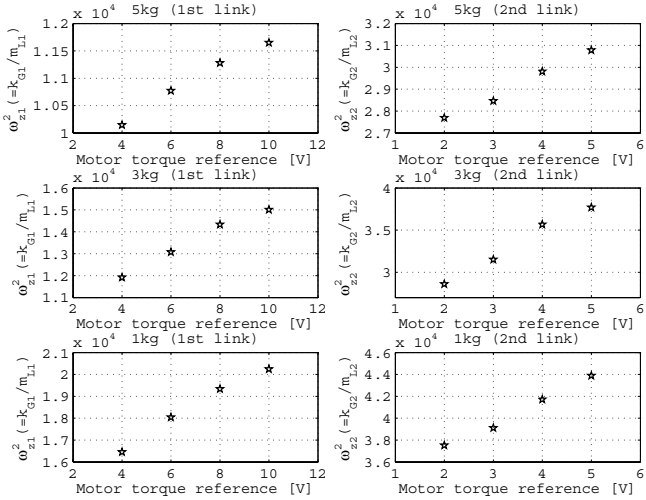

Fig. 15. Plots for squares of estimated anti-resonant angular frequency under changing PRBS-input amplitude. Left: 1st link. Right: 2nd link.